Accepted Manuscript

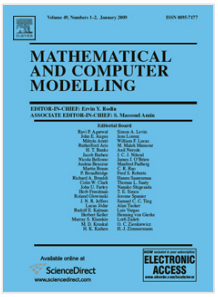

Tumor location and parameter estimation by thermography

J.P. Agnelli, A.A. Barrea, C.V. Turner

PII: S0895-7177(10)00193-7
DOI: 10.1016/j.mcm.2010.04.003
Reference: MCM 4021

To appear in: *Mathematical and Computer Modelling*

Received date: 17 October 2009
Revised date: 23 December 2009
Accepted date: 7 April 2010

Please cite this article as: J.P. Agnelli, A.A. Barrea, C.V. Turner, Tumor location and parameter estimation by thermography, *Mathematical and Computer Modelling* (2010), doi:10.1016/j.mcm.2010.04.003

Tumor location and parameter estimation by thermography

J.P. Agnelli, A. A. Barrea and C. V. Turner *

FaMAF, Universidad Nacional de Córdoba - CIEM-CONICET. Córdoba, Argentina.

Abstract

In non-invasive thermal diagnostics, accurate correlations between the thermal image on skin surface and interior human physiology are often desired, which require general solutions for the bioheat equation. In this study an estimation methodology is presented to determine unknown thermophysical or geometrical parameters of a tumor region using the temperature profile on the skin surface that may be obtained by infrared thermography. To solve these inverse problems a second order finite difference scheme was implemented to solve the bioheat Pennes equation with mixed boundary conditions in 2 and 3 dimensions. Then, the Pattern Search algorithm was used to estimate the different parameters by minimizing a fitness function involving the temperature profiles obtained from simulated or clinical data to those obtained by the finite different scheme.

1 Introduction.

It has long been established that body temperature is an indicator of health. In general the body surface temperature is controlled by the blood circulation underneath the skin, local metabolism, and the heat exchange between the skin and its environment [1–3]. Changes in any of these parameters can induce variations of temperature and heat flux at the skin surface reflecting the physiological state of the human body. The particular tumor architecture and angiogenesis processes can lead to an abnormal situation. Inflammation, metabolic rate, interstitial hypertension, abnormal vessel morphology and lack of response to homeostatic signals are some of the particular features that make tumors to behave differently than normal tissue in terms of heat production and dissipation. Temperatures at skin above a breast tumor or a malignant melanoma, a tumor of melanocytes which are found predominantly in skin, have been found to be several degrees higher than that of the surrounding area [4–7]. So, the abnormal temperature at skin surface can be used in order to predict the location, size and thermal parameters of the tumor region as well as to study the tumor evolution after a treatment procedure.

Medical infrared thermography is non-invasive, non-contact and functional imaging method that measure the radiation emitted from the skin surface and provides information about subtle temperature changes in it. The different patterns of temperature not only depends on physical parameters such as the tissue sensitivity coefficient, but also in the physiology associated to the homeostatic and metabolic processes and the structure and dynamics of the vascular, tissular and nervous systems.

Medical applications of infrared thermography are not a recent phenomenon. However, in the past years their success was rather limited mainly due to the complexity, high cost and poor sensitivity provided by the generation of infrared cameras that were available at that time. Nowadays, advances in the infrared technology have again promoted its medical application as a promising non-invasive tool for imaging the functionality of superficial layers of tissues and the influence of vascular, neurogenic and metabolic process that affect them. In [7] Santa Cruz et al. have investigated by means of thermography the correlation, in patients treated with boron neutron capture therapy (BNCT), between the spatial

*E-mail address: agnelli@famaf.unc.edu.ar, abarrea@famaf.unc.edu.ar, turner@famaf.unc.edu.ar

extension of the acute skin reaction and the superficial dose distribution, in order to better determine tolerance doses and therefore to optimize the BNCT treatment. Also they conclude that given the capacity of thermography to observe the functional aspects of tissues, the technique can help to locate abnormally high temperature regions as well as melanoma nodules that are virtually invisible in CT images.

Further aspect of IR imaging techniques of skin cancer and detection methods from infrared images are describes in detail in a book by Diakides and Bronzino [9].

The objective of this study is the development of a methodology to estimate the depth and size of an embedded malignant melanoma as well as the estimation of the metabolic heat source intensity inside the tumor region. To solve these inverse problems we use temperature profiles on the skin surface that may be obtained by infrared thermography.

Inverse problems are being increasingly used in the development of a lot of applications in different areas of sciences. Some examples are the design of thermal equipments and heat transfer problems [10, 11] in engineering, computerized tomography and image reconstruction [12] in medical imaging and structured population dynamics [13] in biology among others. For works related with thermal diagnosis see [3, 14–17].

After we have introduced the medical facts about the skin cancer and the relation with the temperature of the body, the plan for the rest of this work is the following. In section 2 we show the mathematical model proposed to simulate the heat transfer in a human body in 2D and 3D domains. In Section 3 we present a difference scheme method of order two to discretize the continuous model, the bioheat Pennes equation with the mixed boundary conditions. Also, we show some examples of the solutions in 2D and 3D. In section 4 we present two different inverse problems, one of them associated with the localization of the tumor region and the other one related with the metabolic heat rate. The different results obtained from simulations with and without random noise are exposed. Finally, in section 5 we give some comments and conclusions.

2 Mathematical model.

A number of bioheat transfer equations for living tissues have been proposed since the landmark paper by Pennes [18] appeared in 1948. His main theoretical contribution was the suggestion that the rate of heat transfer between the blood and tissue is proportional to the product of the volumetric perfusion rate and the difference between the arterial blood temperature and the local tissue temperature.

The equation includes the heat transfer by conduction through the tissue, the volumetric metabolic heat generation of the tissue and a term including the volumetric perfusion rate and the difference between the arterial blood temperature and the local tissue temperature, where the arterial temperature is approximated to the core temperature of the body. The Pennes bioheat transfer equation is widely used to solve the temperature distribution for thermal therapy [14–16].

In most of the works related with this topic the following steady-state Pennes equation is considered;

$$\lambda_e \nabla^2 T_e(\mathbf{x}) + k_e[T_b - T_e(\mathbf{x})] + Q_{me} = 0, \quad \mathbf{x} \in \mathbb{R}^n, n = 2,3.$$

where the subscripts $e = 1,2$ identify the sub-domains of healthy tissue and tumor respectively (Fig. 1), λ_e is the thermal conductivity, $k_e = G_{b_e} c_b$ is the perfusion coefficient (G_{b_e} is the blood perfusion rate, c_b is the volumetric specific heat blood), Q_{me} is the metabolic heat source and T_b is the constant blood temperature.

Figure 1: Three dimensional domain. Ω_1 healthy tissue and Ω_2 tumor region.

In this work, instead of considering discontinuous physiological coefficients, we consider, in order to have a more realistic model, smooth coefficients. This was done using [19] and is explained below.

Given the center and the radio R of the tumor we know where the subdomain Ω_2 is located, so we can define a curve γ such that: (i) is contained in Ω_1 and (ii) is exterior to $\partial\Omega_2$ (Fig.2). For simplicity we consider γ as a circumference with the same center that Ω_2 and radio $R+f(R)$, where f is a linear function with positive slope. Then, we define the functions $\rho_e, e=1,2$, with the following properties:

1. $\rho_1(\mathbf{x}) \equiv 0, \quad \mathbf{x} \in \Omega_2$.
2. $\rho_1(\mathbf{x}) \equiv 1, \quad$ everywhere on γ and its exterior.
3. $\rho_1(\mathbf{x}) \quad$ is $\quad C^\infty \quad \mathbf{x} \in \Omega_1 \cup \Omega_2$.

Similarly,

1. $\rho_2(\mathbf{x}) \equiv 1, \quad \mathbf{x} \in \Omega_2$.
2. $\rho_2(\mathbf{x}) \equiv 0, \quad$ everywhere on γ and its exterior.
3. $\rho_2(\mathbf{x}) \quad$ is $\quad C^\infty \quad \mathbf{x} \in \Omega_1 \cup \Omega_2$.

Figure 2: (a)Subdomains Ω_1 and Ω_2. (b)Function ρ_1. (c) Function ρ_2.

Then, for example, we define the thermal conductivity coefficient as:

$$\lambda(\mathbf{x}) = \lambda_1\rho_1(\mathbf{x}) + \lambda_2\rho_2(\mathbf{x}).$$

Doing the same with the rest of the physiological coefficients we obtain the following differential equation:

$$\lambda(\mathbf{x})\nabla^2 T(\mathbf{x}) + k(\mathbf{x})[T_b - T(\mathbf{x})] + Q_m(\mathbf{x}) = 0, \quad \mathbf{x} \in \mathbb{R}^n, n = 2,3. \tag{1}$$

where $\lambda(\mathbf{x}), k(\mathbf{x})$ and $Q_m(\mathbf{x})$ are C^∞ in the whole domain $\Omega = \Omega_1 \cup \Omega_2$. The boundary conditions for this equations are described next.

At the bottom boundary Γ_b, a constant core temperature T_b was assumed:

$$T(\mathbf{x}) = T_b, \qquad \mathbf{x} \in \Gamma_b.$$

The lateral boundary conditions were prescribed as follows:

$$-\lambda(\mathbf{x})\frac{\partial T(\mathbf{x})}{\partial n} = 0, \qquad \mathbf{x} \in \Gamma_l$$

where Γ_l represents the lateral sides for $n=2$ and the lateral facets for $n=3$. The reason for adopting the adiabatic condition on these boundaries is due to the assumption that at positions far from the center of the domain the temperature field is almost not affected by any source located near the center or any external heating or cooling.

Finally, at skin surface, the following convection condition was imposed:

$$-\lambda(\mathbf{x})\frac{\partial T(\mathbf{x})}{\partial n} = \alpha[T(\mathbf{x}) - T_a] \qquad \mathbf{x} \in \Gamma_t,$$

where α is a heat transfer coefficient and T_a is the ambient temperature and $t=4$ in the 2 dimensional case and $t=6$ in the 3 dimensional.

It is possible to consider the evaporation on the skin surface, in that case we have to consider an evolution in time for the heat equation, since the humidity coefficient depends on time.

3 Numerical Method - Direct Problem

To solve the problem presented in the previous section we used a finite difference method (FDM). For simplicity we show how we proceeded in the 2-dimensional case. We considered an equispaced grid on the x and y directions and we approximated the Laplacian by a second order scheme.

To be clear, assume that $\Delta x = \Delta y = h$, in the x-direction $i = 1, ..., n_x$ and in the y-direction $j = 1, ..., n_y$, so we have:

$$(\frac{\partial^2 T}{\partial x^2} + \frac{\partial^2 T}{\partial y^2}) \mid_{i,j} = \frac{T_{i+1,j} - 2T_{i,j} + T_{i-1,j}}{h^2} + \frac{T_{i,j+1} - 2T_{i,j} + T_{i,j-1}}{h^2},$$

then the equation can be rewritten as

$$\lambda_{i,j}(\frac{T_{i+1,j} - 2T_{i,j} + T_{i-1,j}}{h^2} + \frac{T_{i,j+1} - 2T_{i,j} + T_{i,j-1}}{h^2}) + k_{i,j}[T_b - T_{i,j}] + Q_{i,j} = 0,$$

and doing some algebraic operations we obtain

$$T_{i,j} = \frac{\lambda_{i,j}}{4\lambda_{i,j} + h^2 k_{i,j}}(T_{i+1,j} + T_{i-1,j} + T_{i,j+1} + T_{i,j-1}) + \frac{h^2}{4\lambda_{i,j} + h^2 k_{i,j}}(k_{i,j} T_b + Q_{i,j}). \quad (2)$$

Because the partial derivatives in the Laplacian equation were approximated by a second order finite difference scheme, the partial derivatives at the boundaries were also approximated by a second order difference. We accomplished this by considering fictitious grid points outside the domain and then we replaced these fictitious points in the main equation. Here we describe each boundary condition.

At the left lateral boundary we have:

$$\frac{\partial T}{\partial x} \mid_{1,j} = \frac{T_{2,j} - T_{0,j}}{2h} = 0,$$

therefore $T_{0,j} = T_{2,j}$ and replacing this into equation (2) and denoting $\beta_{i,j} = 4\lambda_{i,j} + h^2 k_{i,j}$ we obtain:

$$T_{1,j} = \frac{\lambda_{1,j}}{\beta_{1,j}}(T_{1,j+1} + 2T_{2,j} + T_{1,j-1}) + \frac{h^2}{\beta_{1,j}}(k_{1,j} T_b + Q_{1,j}) \quad j = 2, ..., n_y - 1. \quad (3)$$

In the same way, at the right lateral flux:

$$T_{n_x,j} = \frac{\lambda_{n_x,j}}{\beta_{n_x,j}}(T_{n_x,j+1} + 2T_{n_x-1,j} + T_{n_x,j-1}) + \frac{h^2}{\beta_{n_x,j}}(k_{n_x,j} T_b + Q_{n_x,j}) \quad j = 2, ..., n_y - 1. \quad (4)$$

At the top convective boundary:

$$T_{i,n_y} = \frac{\lambda_{i,n_y}}{\beta_{i,n_y} + 2h\alpha}(2T_{i,n_y-1} + T_{i+1,n_y} + T_{i-1,n_y} + \frac{2h\alpha T_a}{\lambda_{i,n_y}}) + \frac{h^2}{\beta_{i,n_y} + 2h\alpha}(k_{i,n_y} T_b + Q_{i,n_y}), i = 2, ..., n_x - 1. \quad (5)$$

Finally, the bottom boundary condition is:

$$T_{i,1} = T_b \quad i = 2, ..., n_x - 1. \quad (6)$$

We define the sequence $T_{i,j}^{n+1} = F(T_{i,j}^n)$, where F stands for the right hand sides corresponding to the equations (2-6). Given an initial value $T_{i,j}^0$, we compute the values of $T_{i,j}^{n+1}$ through the whole domain

until $max_{i,j} e(i,j) < \varepsilon$, where $e(i,j)$ is the relative error at (i,j) defined as $e(i,j) = \frac{|T_{i,j}^{n+1} - T_{i,j}^{n}|}{T_{i,j}^{n}}$ and ε the desired tolerance error.

To show how the proposed numerical method works, we present some solutions of equation (1) and the respective boundary conditions. In all cases the following thermal physiological parameters have been assumed [14–16]: $\lambda_1 = 0.5[W/mK]$, $\lambda_2 = 0.75[W/mK]$, $k_1 = 1998.1[W/m^3K]$, $k_2 = 7992.4[W/m^3K]$, $Q_{m1} = 4200[W/m^3]$, $Q_{m2} = 42000[W/m^3]$, $T_b = 37°C$, $T_a = 25°C$, $\alpha = 10[W/m^2K]$ and a step $h = 6 * 10^{-4}[m]$.

For the 2 dimensional examples the dimensions of the domain were 0.09 x 0.03$[m]$ and in this particular first example, the center of the tumor was assumed at $(0.045, 0.020)$ and the radius was $0.005[m]$. In figure 3*a* we can see the temperature distribution over the whole domain, it starts at $37°C$ at the bottom and decreases, due to the convective condition at the skin surface, but it has an important increase in the region where the tumor is located. Figure 3*b* shows the temperature profile on the skin surface, we see a difference in temperature of almost $1°C$ degree between the region that is above the tumor and regions that are away from it. This agrees with the idea that the presence of a highly vascularized tumor can lead to the increase of temperature at skin surface.

Figure 3: (a)Temperature distribution. (a)Temperature profile on the skin surface.

In figure 4 we present another 2 dimensional example. Here the center of the tumor was assumed at $(0.030, 0.022)$ and the radius is equal to $0.004[m]$. Figure 4*a* shows the temperature profile over the whole domain and figure 4*b* the temperature profile on the skin surface. Again, we can see there is a difference of almost $1°C$ between the area located above the tumor and areas that are further away.

Figure 4: (a)Temperature distribution. (b)Temperature profile on the skin surface.

For the 3 dimensional case, we present two examples showing the proposed methodology. In both examples we assumed a domain of dimension 0.09 x 0.09 x 0.03$[m]$. In the first example the location center was assumed at $(0.045, 0.045, 0.002)$ and the radius is equal to $0.06[m]$. In figure 5 we see the temperature profile on the skin surface. This figure reveals a difference of $0.5°C$ between areas above the tumor and areas above healthy tissue.

Figure 5: Temperature profile on the skin surface.

Figure 6 shows another 3 dimensional example. In this case the tumor center was assumed at $(0.06, 0.06, 0.02)$ and the radius is equal to $0.006[m]$.

Figure 6: Temperature profile on the skin surface.

4 Inverse Problem and Results

According to [4, 5, 8], the presence of a highly vascularized tumor can lead to the increase of local blood perfusion and the capacity of metabolic heat source and therefore this causes an increase of temperature at the skin surface. Then, the idea is to use the abnormal temperature at skin surface in order to predict the location, size and thermal parameters of the tumor, this has been done considering two different inverse problems. The first problem concerns in the localization; depth, width and size of the tumor, assuming that all others parameters are known. The second one, is related with the estimation of the metabolic heat source intensity inside the tumor region being known the location of the center and the radius of the tumor.

In both cases we used the same methodology. Given temperature profiles obtained from the simulations, these were used as the clinical data. Then the Pattern Search method [20–23], was used to estimate the tumor parameters by minimizing a fitness function. The fitness function relates the given data to the temperature profile for a given set of estimated parameters. For the first problem it was defined as:

$$E = \|T_{obs} - T_{num}(x, y, R)\|_2,$$

where T_{obs} is the observed temperature and T_{num} is the estimated skin temperature obtained with the FDM using the parameters (x, y, R). For the second problem the fitness function was defined in a similar way. In both problems some linear constraints were considered during the minimization process. These constraints are related with the geometry of the tumor and with the physiological parameters values.

Here we present some results we have obtained. These results show that for the 2 dimensional case, as well as for the 3 dimensional case, it is possible to determine the required parameters from the surface temperature data. Moreover when 5% and 10% of random noise was added to the input data the results obtained were very good. In the case when the input data were contaminated with 15% of random noise the results obtained were good enough. In all cases the values of the known parameters and the dimensions of the domain were the same as in section (3). We emphasize we have run the algorithm several times using different initial random conditions and in all cases the results were similar.

Table 1 shows the results for the inverse problem related with the tumor location in 2 dimensions. Here, we see that using the proposed methodology it is possible to determine the location and radius of the tumor with a good accuracy.

The results obtained for the estimation of the metabolic heat source intensity in the two dimensional problem are shown in table 2. Again, we see a good agreement between actual and predicted parameter.

Original data			without noise			10% noise			15% noise		
x	y	R	x	y	R	x	y	R	x	y	R
0.040	0.020	0.003	0.0400	0.0209	0.0003	0.0403	0.0203	0.0029	0.0399	0.0215	0.0028
0.020	0.015	0.004	0.0206	0.0158	0.0039	0.0199	0.0162	0.0038	0.0195	0.0168	0.0045
0.029	0.020	0.005	0.0289	0.0204	0.0050	0.2900	0.0193	0.0051	0.0286	0.0204	0.0048

Table 1: Estimation of the center and the radius of the tumor in 2D. The different columns show the results obtained considering data without random noise and data with random noise of 10% and 15% respectively.

Original Data		without noise	10% noise	15% noise
Q_2	42000	42000	41881.17	42537.18
Q_2	37000	37000	37177.50	37632.90
Q_2	25000	25000	24891.71	25716.82

Table 2: Estimation of the metabolic heat source intensity in 2D. In all cases the center was assumed at $(0.045, 0.02)$ and the radius equal to 0.005.

Table 3 shows the results related with the first inverse problem but in this case in 3 dimensions. It should be noted that in this case the algorithm is time consuming.

Finally, table 4 shows the results obtained for the estimation of the metabolic heat source intensity inside the tumor region. This problem is of our interest because the estimation of thermophysical parameters related with a tumor could be useful and important to study the tumor evolution after a cancer treatment like the BNCT [7]. Comparison of the heat source intensity Q_2 inside the tumor, before and after the treatment, could be used as a measure to evaluate the effectiveness of the cancer treatment.

Remark : It's worth noting that the good results obtained are largely due to the strong restrictions imposed to the class of functions allowed for the thermal coefficients and the metabolic heat source. This can be taken in the sense of regularization by discretization [24]. The restriction imposed on the family of functions implies a reduction in the dimension of the space of solutions.

5 Conclusions and future work

A simple methodology was developed for the estimation of thermophysical or geometrical parameters of a tumor region using the temperature profile on the skin surface that may be obtained by infrared thermography. These inverse problems have been solved using a second order finite difference scheme coupled with the Pattern Search algorithm. The presented results demonstrate the feasibility of the pro-

Original Data		without noise	noise 10%	noise 15%	Original Data		without noise	noise 10%	noise 15%
x	0.030	0.0301	0.0304	0.2989	x	0.020	0.0201	0.0198	0.0191
y	0.030	0.0300	0.0298	0.0303	y	0.015	0.0155	0.0156	0.0159
z	0.022	0.0221	0.0223	0.0231	z	0.019	0.0189	0.0179	0.0160
R	0.005	0.0050	0.0049	0.0048	R	0.006	0.0059	0.0063	0.0069

Table 3: Estimation of the center and the radius of the tumor in 3D. The different columns show the results obtained considering data without random noise and data with random noise of 10% and 15% respectively.

Original Data		without noise	10% noise	15%noise
Q_2	42000	42000	41690.09	40741.71
Q_2	37000	37000	37957.31	36675.37
Q_2	25000	25000	24609.03	26307.50

Table 4: Estimation of the metabolic heat source intensity 3D. In all cases the center was assumed at $(0.045, 0.045, 0.015)$ and the radius equal to 0.005.

posed methodology. Even in the case when 5% and 10% of noise was added to the input data the methodology estimates the different parameters with very good accuracy for the 2D case as well as for the 3D case.

The good results obtained are largely due to the strong restrictions imposed to class of functions allowed for the thermal coefficients and the metabolic heat source.

According to the results, this methodology can help to locate tumor regions, like melanoma nodules, as well as to estimate parameters related with them that could be useful and important to study the tumor evolution after a treatment procedure.

As future work we plan to focus on the regularization of the problem considering different regularization methods and iterative algorithms. In order to solve the optimization problem, we will use an algorithm that take in account the derivative of the functional like the conjugate gradient method.

Acknowledgments

The work of the authors was partially supported by grants from CONICET, SECYT-UNC and PICT-FONCYT. The authors want to thank Gustavo Santacruz and Sara González for the motivation to connect this work with the Boron Neutron Capture Therapy in which they have been working at the CNEA and the Roffo Hospital. We also thank to the referees for all the helpful comments.

References

[1] **J. C. Chato**. Measurement of thermal properties of biological materials,in: A. Shitzer, R.C. Eberhart (Eds.), Heat Transfer in Medicine and Biology, vol I, Plenum Press,NY, 1985, pp.167-173.

[2] **H. F. Bowman**. Estimation of tissue blood flow, in: A. Shitzer, R.C. Eberhart (Eds.), Heat Transfer in Medicine and Biology, vol I, Plenum Press,NY, 1985, pp.193-230.

[3] **M. M. Chen, C. O. Pedersen and J. C. Chato**. On the feasibility of obtaining three dimensional information from thermographic measurements. ASME Journal of Biomechanical Engineering, 99, 1977, pp.58-64.

[4] **R. N. Lawson**. Implications of surface temperatures in the diagnosis of breast cancer. Canadian Medical Asociation Journal, vol. 75, 1956, pp.309-310.

[5] **R. N. Lawson and M.S. Chugtai**. Breast cancer and body temperatures. Canadian Medical Asociation Journal, vol. 88, 1963, pp.68-70.

[6] **M. Miyakawa and J.C. Bolomey**(Eds). Non-Invasive Thermometry of the Human Body. CRC Press, Boca Raton, 1996.

[7] **G. A. Santa Cruz, J. Bertotti, J. Marín, S.J. González, S. Gossio, D. Alvarez, B.M.C. Roth, P. Menéndez, M.D. Pereira, M. Albero, L. Cubau, P. Orellano and S.J. Liberman**. Dynamic

infrared imaging of cutaneous melanoma and normal skin in patients treated with BNCT. Appl. Radiat.Isotopes, vol. 67,pp s54-s58, 2009.

[8] **M. Gautherie**. Clinical Thermology. Subseries Thermotherapy, vol. 1-4, Springer-Verlag, Heidelberg,1990.

[9] **N.A. Diakides and J.D. Bronzino**. Medical infrared imaging. CRC Press, Boca Raton, Florida, USA, 2007.

[10] **J. Su and A. J. Silva Neto** . Two-dimensional inverse heat conduction problem of source strength estimation in cylindrical rods. Applied mathematical Modelling, 25, 2001, pp. 861-872.

[11] **A. J. Silva Neto and M.N. Ozisik**. Simultaneous estimation of location and timewise-varying strength of a plane heat source. Num. Heat Transfer, Part A: Applications, 25, 1993, pp. 467-477.

[12] **J. P. Zubelli, R. Marabini, C. O. S. Sorzano and G. T. Herman**. Three- dimensional reconstruction by Chahine's method from electron microscopic projections corrupted by instrumenstal aberrations. Inversae Problems , 19,2003, pp. 933-949.

[13] **B. Perthame and J. P. Zubelli**. On the inverse problem for a size structured population model. Inversae Problems , 23, 2007, pp. 1037-1052.

[14] **Z. Deng and J. Lui**. Mathematical modelling of temperature over skin surface and its implementation in thermal disease diagnostics. Computers in Biology and Medicine, 34, 2004, pp.495-521.

[15] **M. Paruch and E. Majchrzak**. Identification of tumor region parameters using evolutionary algorithm and multiple reciprocity boundary element method. Enginnering Applications of Artificial Intelligence, 20, 2007, pp.647-655.

[16] **M. Mital and Elaine P. Scott**. Thermal Detection of Embedded Tumors using Infrared Imaging. ASME Journal of Biomechanical Engineering, vol. 129 (1),2007, pp.33-39.

[17] **J. Lui and L.X. Xu**. Boundary information based diagnostics on the thermal states of biological bodies. Int. J. of Heat and Mass Transfer, 43, 2000, 2827-2839.

[18] **H. Pennes**. Analysis of tissue and arterial blood temperature in the resting human forearm J. Appl. Physiol. 1, 1948, pp.93-122.

[19] **J. Boyd**. Fourier embedded domain methods: extending a function defined on an irregular region to a rectangle so that the extension is spatially periodic and C^{∞}. App. Math. and Computation, 161, 2005, pp.591-597.

[20] **J. Dennis and V. Torczon**. Derivative free pattern search method for multidisciplinary design problems. Proceedings of AIAA, vol. 94, 2001, pp.1-11.

[21] **V. Torczon**. On the convergence of Pattern Search Algorithms. SIAM Journal on Optimization, Vol. 7, Number 1,pp. 1-25, 1997, pp.1-25.

[22] **R.M. Lewis and V. Torczon**. Pattern Search Algorithms for Bound Constrained Minimization. SIAM Journal on Optimization, Vol. 9, Number 4, 1999, pp. 1082-1099.

[23] **R.M. Lewis and V. Torczon**.Pattern Search Methods for Linearly Constrained Minimization. SIAM Journal on Optimization, Vol. 10, Number 3, 2000, pp. 917-941.

[24] **H. W. Engl, M. Hanke and A. Neubauer**. Regularization of inverse problems. Kluwer Academic Publisher, Dordchet, 1996.

Figure1

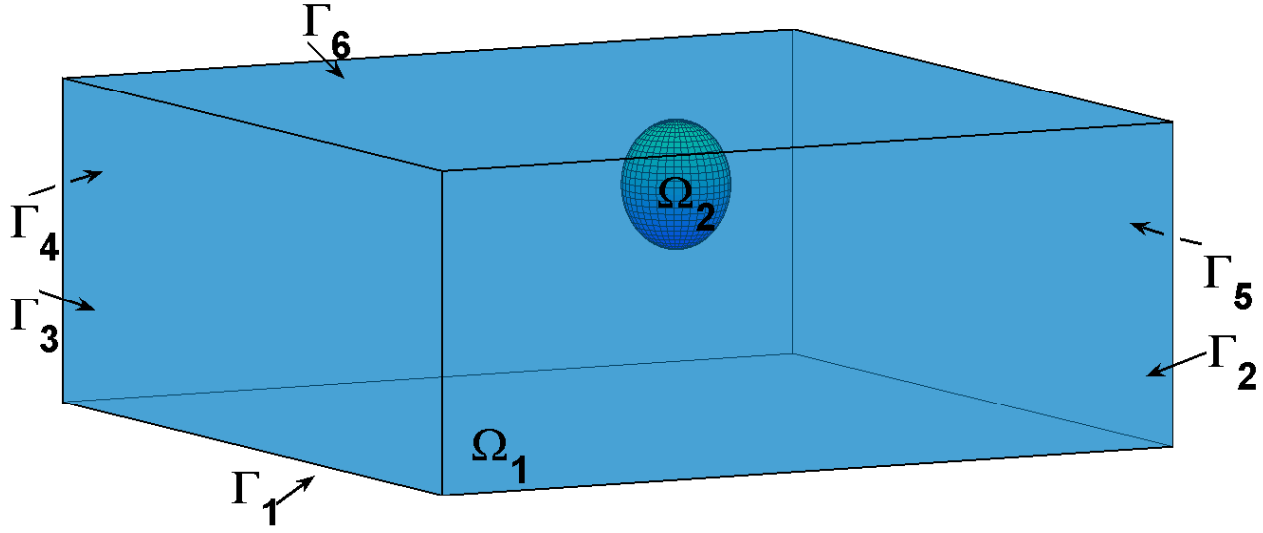

Figure2 (a)

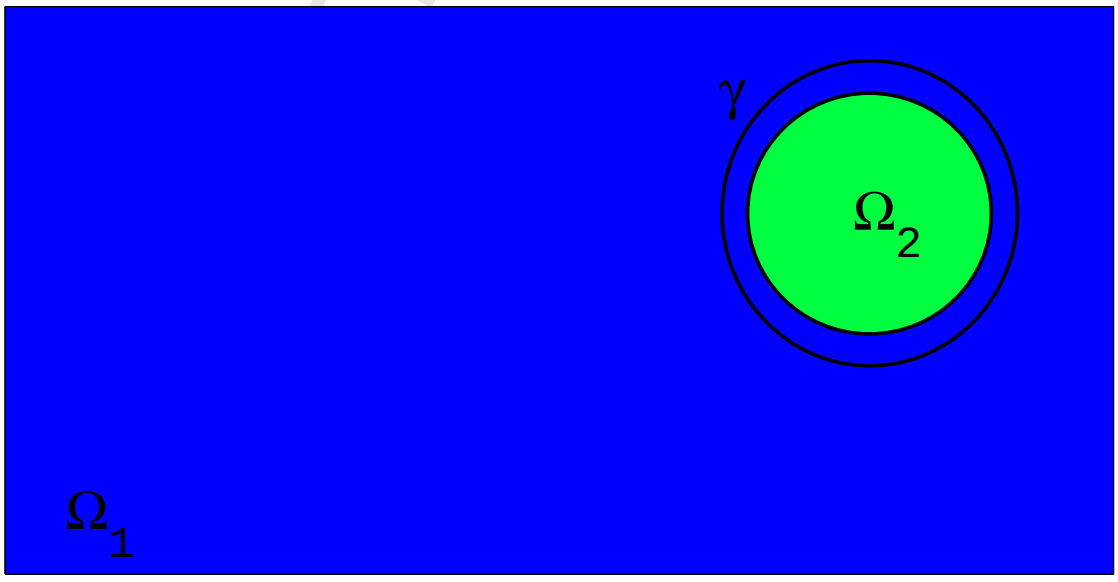

Figure2 (b)

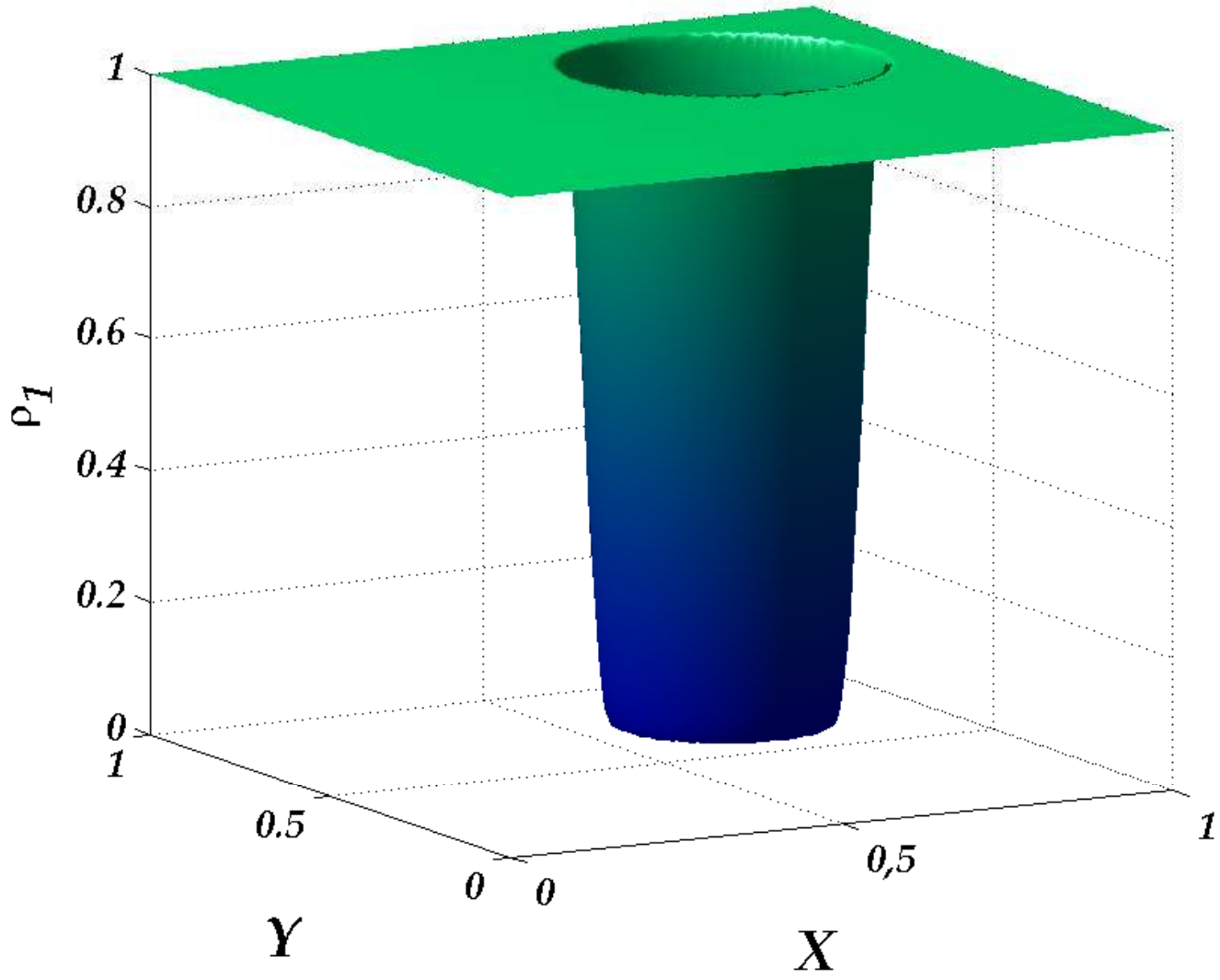

Figure2 (c)

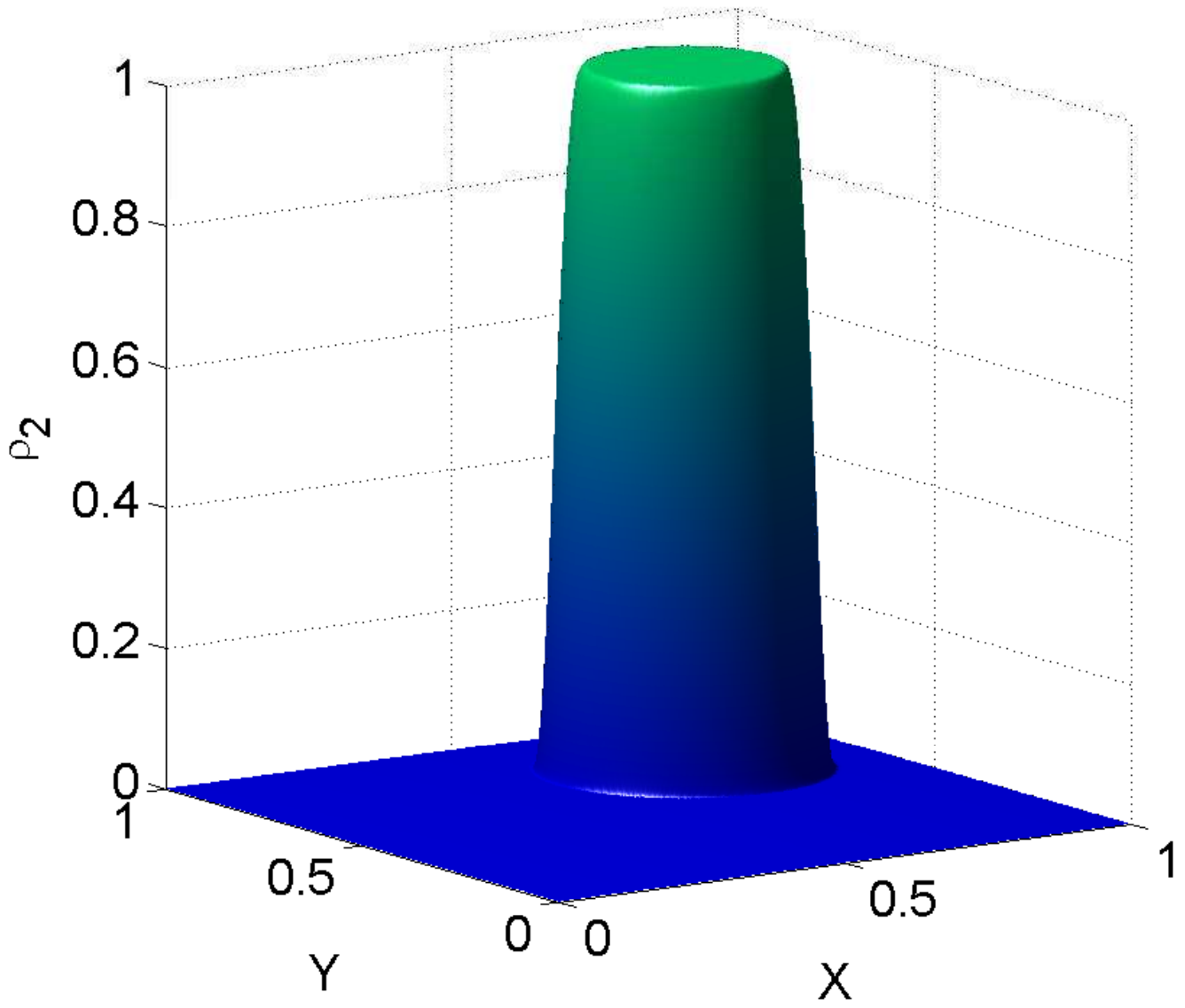

Figure3 (a)

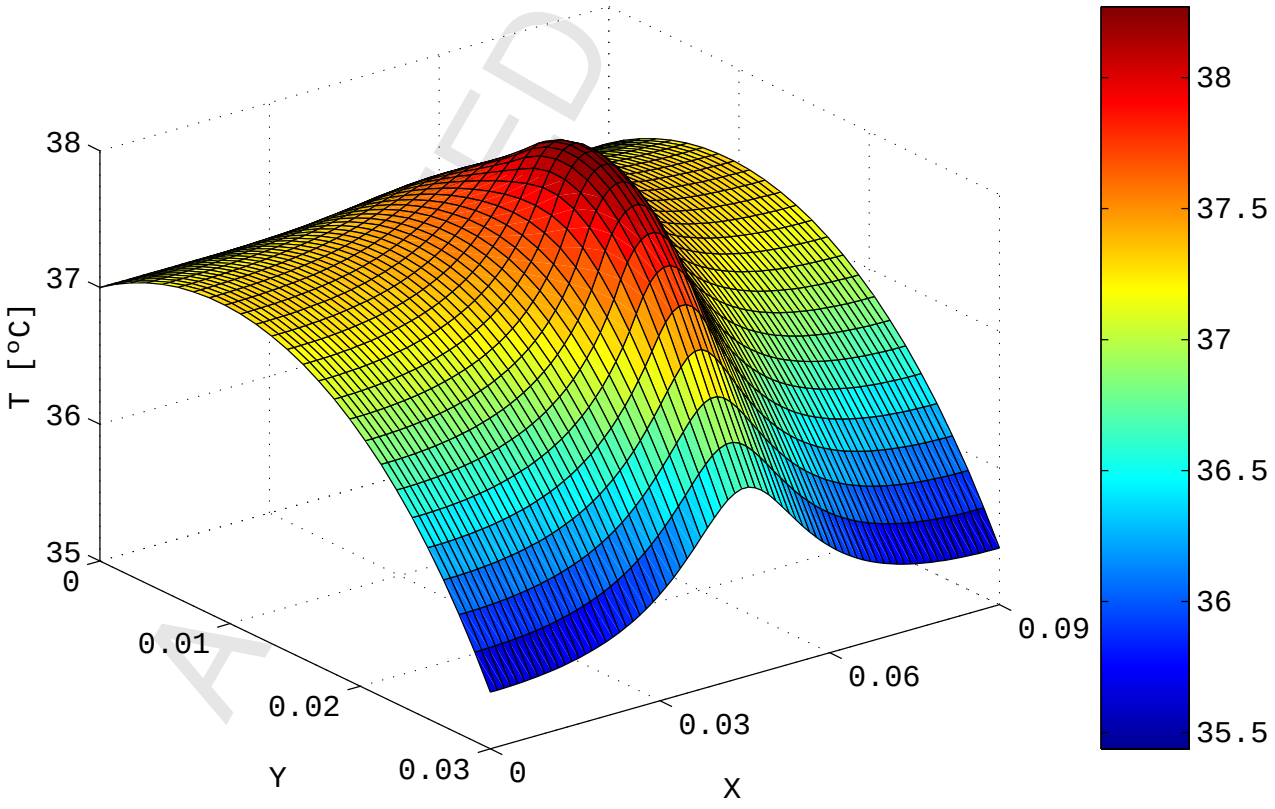

Figure3 (b)

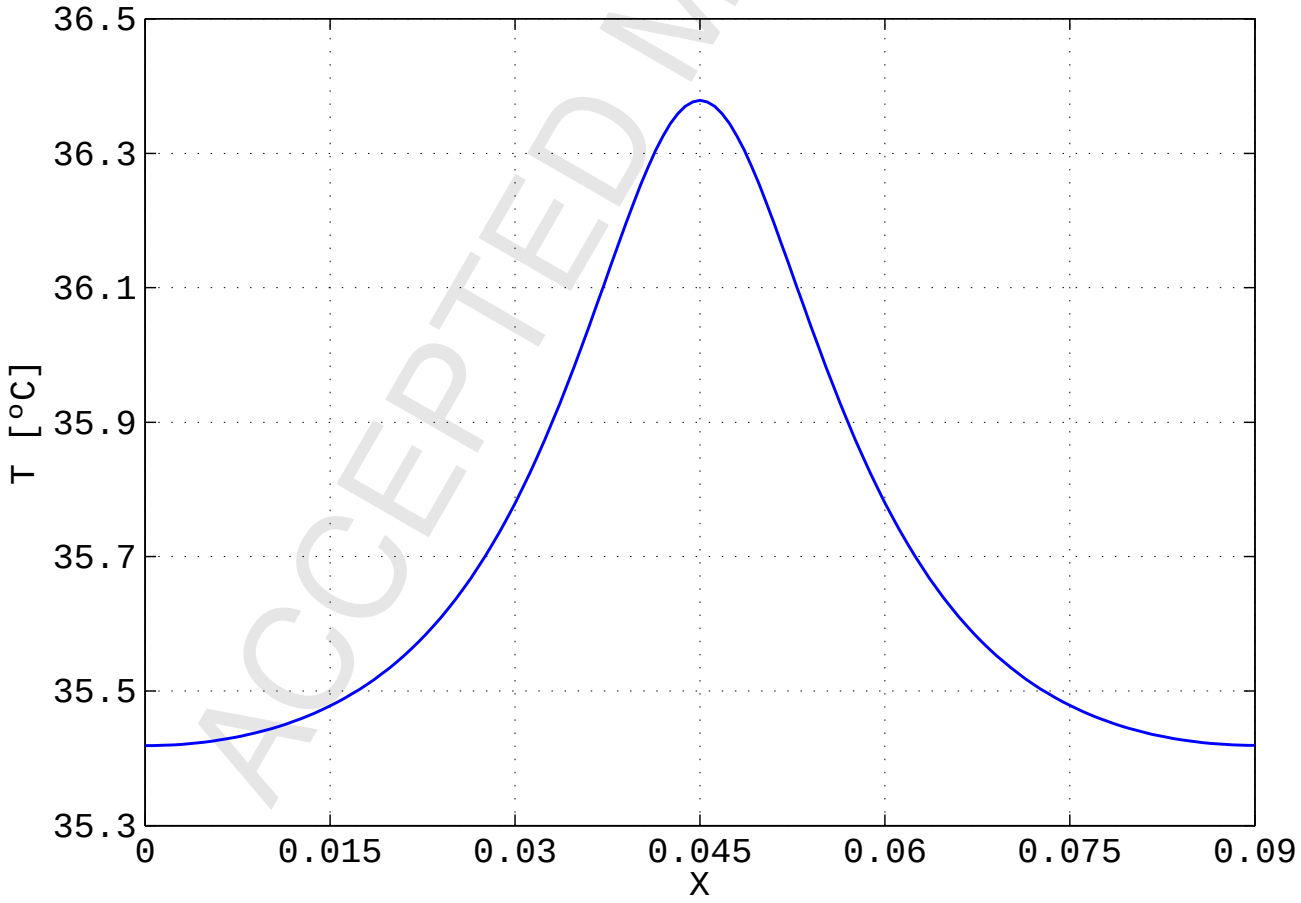

Figure4 (a)

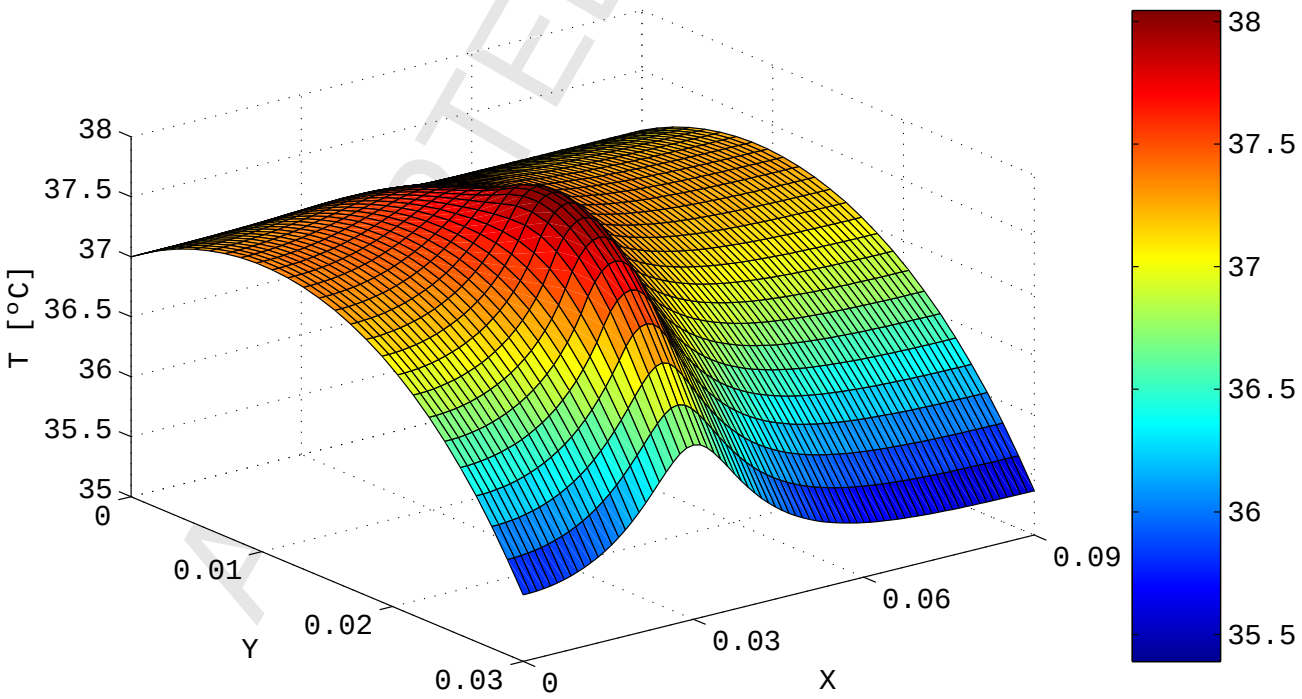

Figure4 (b)

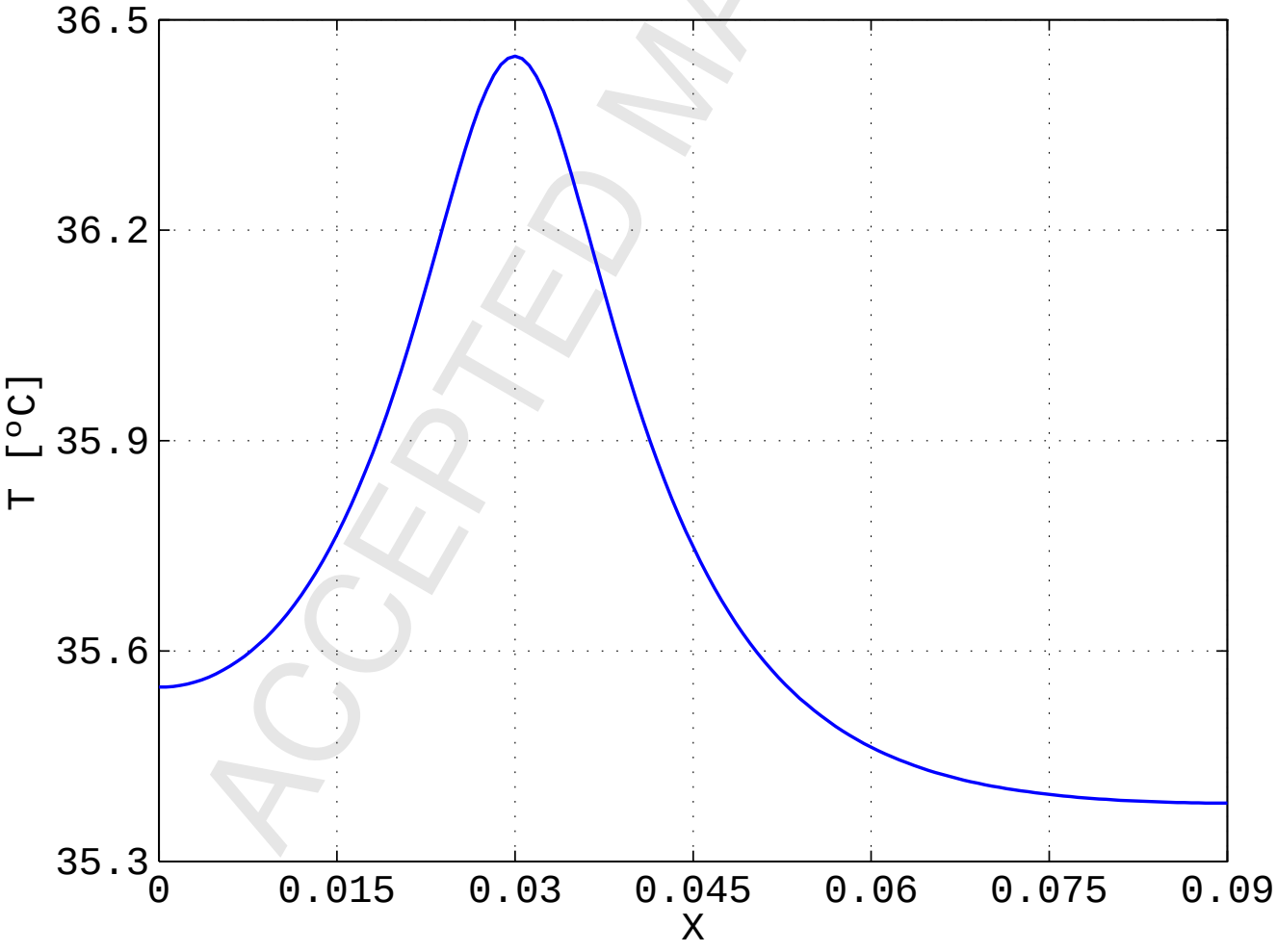

Figure5

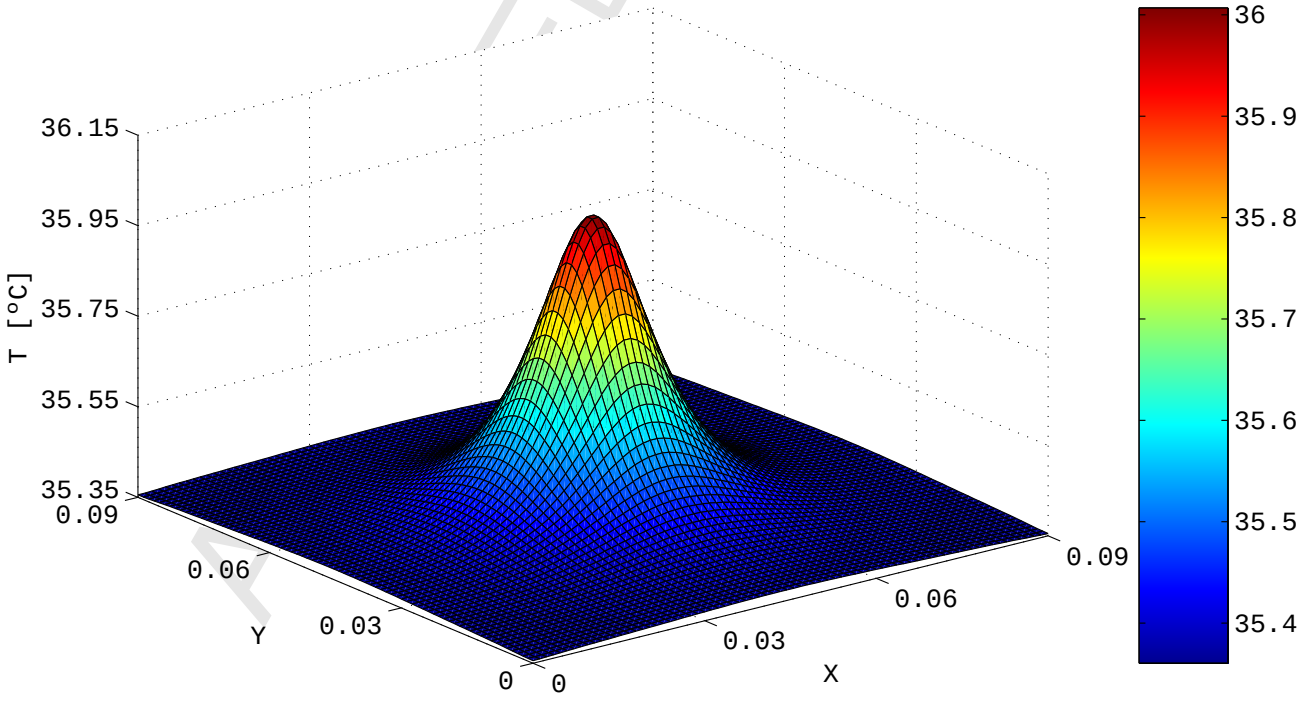

Figure6